

Fugitive natural gas emissions in York, United Kingdom: Updating the parameters of existing algorithms to be based on instrumental limitations.

Thomas C. Moore¹, James R. Hopkins^{1,2}, Will S. Drysdale^{1,2}, Stuart Young¹, Sri Hapsari Budisulistiorini¹, Marvin D. Shaw^{1,2}, Mackenzie LeVernois³, James L. France^{3,4}, David Lowry³ and James D. Lee^{1,2}

¹Wolfson Atmospheric Chemistry Laboratories, University of York, York YO10 5DD, United Kingdom

²National Centre for Atmospheric Science, University of York, York YO10 5DD, United Kingdom

³Royal Holloway, University of London, Earth Sciences, Egham, United Kingdom

⁴Environmental Defence Fund Europe, Avenue des Arts 47-49, Brussels, Belgium

Correspondence to: james.lee@york.ac.uk

Abstract

Reducing methane (CH_4) emissions has become increasingly important in recent years due to its importance for radiative forcing. Fugitive emissions of CH_4 from natural gas distribution infrastructure are of particular interest as a mitigation target within the oil and gas sector. One area of particular interest is the oil and gas sector, which often results in fugitive emissions of methane from natural gas distribution. Previous studies have shown the ability to detect these emissions by use of mobile surveys measuring ~~(CH_4)methane~~. Some of these previous studies use ratios to secondary co-emitted compounds as a means of predicting the source of emission. This study aims to adapt existing algorithm parameters by investigating the limitations of equipment within the platform used for mobile surveys. These changes suggest that previous methods may underpredict the number of Leak Indications (LIs) by 53.5 % with 27 LIs detected with the old methodology compared to 58 LIs detected with the new methodology, the number of LIs detected with the old methodology being 27 and the new methodology detecting 58. The majority of these LIs were found to be emitting in a leak rate category of 0 - 2 L min⁻¹. Source ~~appointment~~ determination was included as a core step within the algorithm ~~itself, which this stage~~ was shown to reduce the misassignment of LIs, suggesting that when not using this step, the previous methodology may include emissions from pyrogenics and biogenics are included within ~~their~~ LI assignments.

28 1 Introduction

29 Following COP26 and the ~~Global Methane Pledge~~~~methane pledge~~ (European Commission and United States of America
30 2021), ~~CH₄ methane~~ and its emissions have received increased attention. The pledge states that the signatories will attempt to
31 reduce their ~~CH₄ methane~~ emissions by 30 % of their 2020 levels by 2030. This was brought about due to increasing concern
32 over the potency of ~~CH₄ methane~~ as a greenhouse gas, with its warming potential 28 times greater than CO₂ over a 100-year
33 timescale and 84 times ~~higher-greater~~ over a 20-year timescale (IPCC, 2021). ~~Anthropogenic sources are estimated to~~
34 ~~contribute to~~ 65 % of all ~~CH₄ methane~~ emissions, ~~with -are thought to be anthropogenic in nature and~~ atmospheric
35 ~~CH₄ methane has seen~~ a consistent growth rate of > 5 ppb year⁻¹ since 2007, with 2021 and 2022 seeing growth rates of
36 17.8 ppb year⁻¹ and 14 ppb year⁻¹ respectively (Saunio *et al.*, 2025). ~~T~~therefore, understanding and mitigating
37 anthropogenic ~~CH₄ methane~~ is a key ~~goal-step in to~~complying with the ~~G~~lobal ~~M~~ethane ~~P~~ledge.

38
39 Of ~~the~~ anthropogenic emissions, the agricultural sector has the largest contribution towards atmospheric emissions (Saunio
40 *et al.*, 2025). Although there are means of reducing these ~~se~~ emissions, ~~from these areas, including changing such as changes to~~
41 cattle, crop ~~and~~ land management as well as changing the feedstock of the cattle, ~~for example from~~ grass silage to maize
42 silage (Bačėninaitė *et al.*, 2022; Nisbet *et al.*, 2025). ~~T~~hese changes may still require time to implement, so this sector
43 cannot be the sole focus in order to reach the 2030 deadline.

44
45 After agriculture, the largest ~~contribution-contributor~~ to anthropogenic emissions is ~~from~~ the energy sector, with oil, natural
46 gas and coal having relatively similar contributions to ~~CH₄ methane~~ emissions. Natural gas is of particular importance to the
47 ~~United Kingdom (UK), with it being which is~~ the 19th largest country emitter of ~~CH₄ methane~~ from the natural gas network
48 (Scarpelli *et al.*, 2022).

49
50 One of the ~~major~~ sources of ~~CH₄ methane~~ emissions from the natural gas network is fugitive emissions. A fugitive emission
51 is an unexpected or unwanted emission of gas from a pressurised network that is not detected by standard means (Sotoodeh,
52 2021). Within the natural gas network, they are commonly referred to ~~colloquially~~ as “~~g~~Gas ~~L~~eaks”. ~~H~~owever, the stigma
53 surrounding this term, both from industrial operators and the public, means the term fugitive emission is preferable to be
54 used where possible.

55
56 In the ~~United Kingdom-UK~~ in 2023, 63.5 billion cubic metres of natural gas was consumed (Energy Institute, 2024). This is
57 used in a range of applications including; industrial use, electricity generation and domestic use. Of the UK’s natural gas
58 consumption, 33.8 % is from the domestic sector (DESNZ, 2024), with 73.8 % of households in England and Wales using
59 mains gas for either heating or cooking purposes (Stewart *et al.*, 2024). In 2022, it was estimated that 117 kT of ~~CH₄ methane~~
60 was emitted as a result of fugitive emissions related to natural gas distribution (NAEI, UK Emissions Data Selector).

61 Within the UK, after natural gas is either produced or imported, it is first transported through ~~the~~ National Gas' National
62 Transmission System (NTS), a network of over 5,000 miles of high-pressure steel pipes and more than 500 above ground
63 installations. ~~This n~~ Natural gas is then transported by one of ~~several of~~ the UK's Gas Distribution Networks (GDNs), a GDN
64 first reduces the pressure from the NTS then oversees the pipework for pre-meter distribution of natural gas to homes and
65 businesses. The GDN responsible for York covers 2.7 million homes and businesses across the northeast of England and
66 northern Cumbria, ~~which means the operation of resulting in~~ tens of thousands of kilometres of pipework and therefore large
67 ~~unknowns-uncertainties~~ in the locations of fugitive emissions. To combat this, previous studies have implemented mobile
68 measurement approaches centred around the detection of areas with elevated CH₄methane.

69 1.1 Previous Mobile Measurement Methodology

70 ~~There have been many~~ Multiple previous studies ~~that~~ have attempted to design algorithms to detect fugitive emissions of
71 natural gas, all of which focus on locating enhancements in CH₄, the major component of natural gas. These algorithms
72 define an enhancement based on whether CH₄ mixing ratios are higher than a certain value (*Phillips et al., 2016*), ~~are~~ above a
73 certain percentile in measured readings (*Hopkins et al., 2016, Chamberlain et al., 2016*) or by using an outlier detection
74 model (*Keyes et al., 2020*).

75
76 The paper upon which our methodology is based, (*von Fischer et al., 2017*), defines Observed Peaks (OPs) as CH₄methane
77 enhancements > 110% of a 2.5-minute rolling background of the mean CH₄ concentrations two minutes before and after
78 each measured point, ~~and that they occur over less than~~ Additionally, OPs must not cover a distance greater than 160 m.
79 Enhancements occurring within 5 seconds of each other are grouped together. Mobile surveys are repeated multiple times
80 and Leak Indications (LIs) are determined ~~after by~~ grouping OPs that occur within 20 m of one another and ~~seeing~~
81 determining which of these grouped clusters contain OPs from more than one mobile survey. The LIs are then quantified into
82 emission rates in L min⁻¹, using an equation derived from the results of a controlled release experiment, shown in *Equation*
83 *1*.

$$84 \quad (\text{release rate} / \text{L min}^{-1}) = 0.1178 + 0.08267 \times M - 0.005175 \times A + 0.08626 \times K \quad (\text{Eq. 1})$$

85 Where:

- 86 - M is the maximum CH₄ reading
- 87 - A is the peak area in ppm.metres
- 88 - K is the ratio of ppm.metres to maximum CH₄

89 This methodology was ~~then~~ further developed in (*Weller et al., 2019*), ~~This changed where~~ the baseline ~~such that it was~~
90 became the median CH₄ value over 2.5 minutes, the spatial grouping of OPs to LIs changed from 20 m to 30 m and the
91 quantification equation changed to *Equation 2*.

$$92 \quad \ln(\text{excess CH}_4 / \text{ppm}) = -0.988 + 0.817 \times \ln(\text{emission rate} / \text{L min}^{-1}) \quad (\text{Eq. 2})$$

93 Where the excess CH₄ term is the mean of all CH₄ enhancements associated with the resulting LI.

94 In (*Maazallahi et al., 2020*), it was proposed that the existing methodology categorised certain burning emissions as fugitive
95 emissions. To counter this, an additional stage using CO₂ ratios with CH₄ was introduced to filter out burning emissions.
96 Source attribution was also used in (*Fernandez et al., 2022*), using isotopic measurements of CH₄ in addition to ethane:
97 methane (C₂:C₁) ratios.

98 Most recently in (*Tettenborn et al., 2025*), the approach was changed further, adapting the quantification equation to be
99 based on peak area as opposed to peak height. Resulting in the quantification equation shown in **Equation 3**.

$$(release\ rate / L\ min^{-1}) = exp(1.292 \times ln(peak\ area) - 2.377) \quad (Eq. 3)$$

101 Where $ln(peak\ area)$ is the mean $ln(peak\ area)$ of all OPs within the LI cluster.

102 Variations of this algorithm have been used in many major cities across the USA and Canada (*Ars et al., 2020; Weller et al.,*
103 *2022*) ~~as well as European cities~~ Europe (*Defratyka et al., 2021; Fernandez et al., 2022; Wietzel et al., 2023; Vogel et al.,*
104 *2024*) and Asian ~~cities~~ (*Joo et al., 2024, Ueyama et al., 2025, Umezawa et al., 2025*). This paper attempts to detect smaller
105 enhancements of methane by adapting detection and clustering parameters to be specific to the limitations of the
106 instrumentation used. The paper also explores the effect of introducing a source attribution filter at the OP stage of the
107 algorithm and how this affects the number and the magnitude of LIs.

108 **2 Methodology**

109 **2.1 Instrumentation**

110 The Wolfson Atmospheric Chemistry Laboratories (WACL) Air Sampling Platform (WASP) detailed in (*Wagner et al.,*
111 *2021*) is the base for these measurements. The sampling inlet for the WASP is located at the front of the van on the driver's
112 side, meaning that the vehicle will sample the centre of the road regardless of direction of travel. Since publication of
113 (*Wagner et al., 2021*), the WASP has been updated to include a Quark-Elec QK-AS07-0183 for GPS readings. For the
114 measurements surrounding natural gas, the WASP was equipped with a Los Gatos Microportable Greenhouse Gas Analyser
115 (MGGA) for measurements of methane and CO₂, Iterative Cavity Enhanced Differential Optical Absorption
116 Spectrometer (ICAD) for measurements of NO_x (NO₂ + NO), and an Aerodyne Tuneable Infrared Laser Direct Absorption
117 Spectrometer (TILDAS) Laser Trace Gas Analyser for measurements of ethane (C₂H₆) (*Yacovitch et al., 2014*).
118 Measurements of C₂H₆ ethane are calibrated using a three point calibration of a high standard ~~of ethane~~ (17.5 ppb), medium
119 (2.5 ppb) and a zero, where calibration standard concentrations were confirmed via GC-MS. For each mobile survey a
120 calibration ~~is was~~ performed before and after the mobile survey itself, a linear regression ~~is was~~ performed to find the slope
121 and intercept of the calibration concentrations versus measured concentrations. The average ~~is taken for of~~ the two
122 calibrations was taken to account for instrument drift during the mobile survey and the resulting equation, **Equation 4**, is was
123 then used to apply a correction to C₂H₆ ethane concentrations.

124

$$125 \quad C_2H_6\ corrected = C_2H_6\ uncorrected \cdot m + c \quad (Eq.4)$$

126 Where:

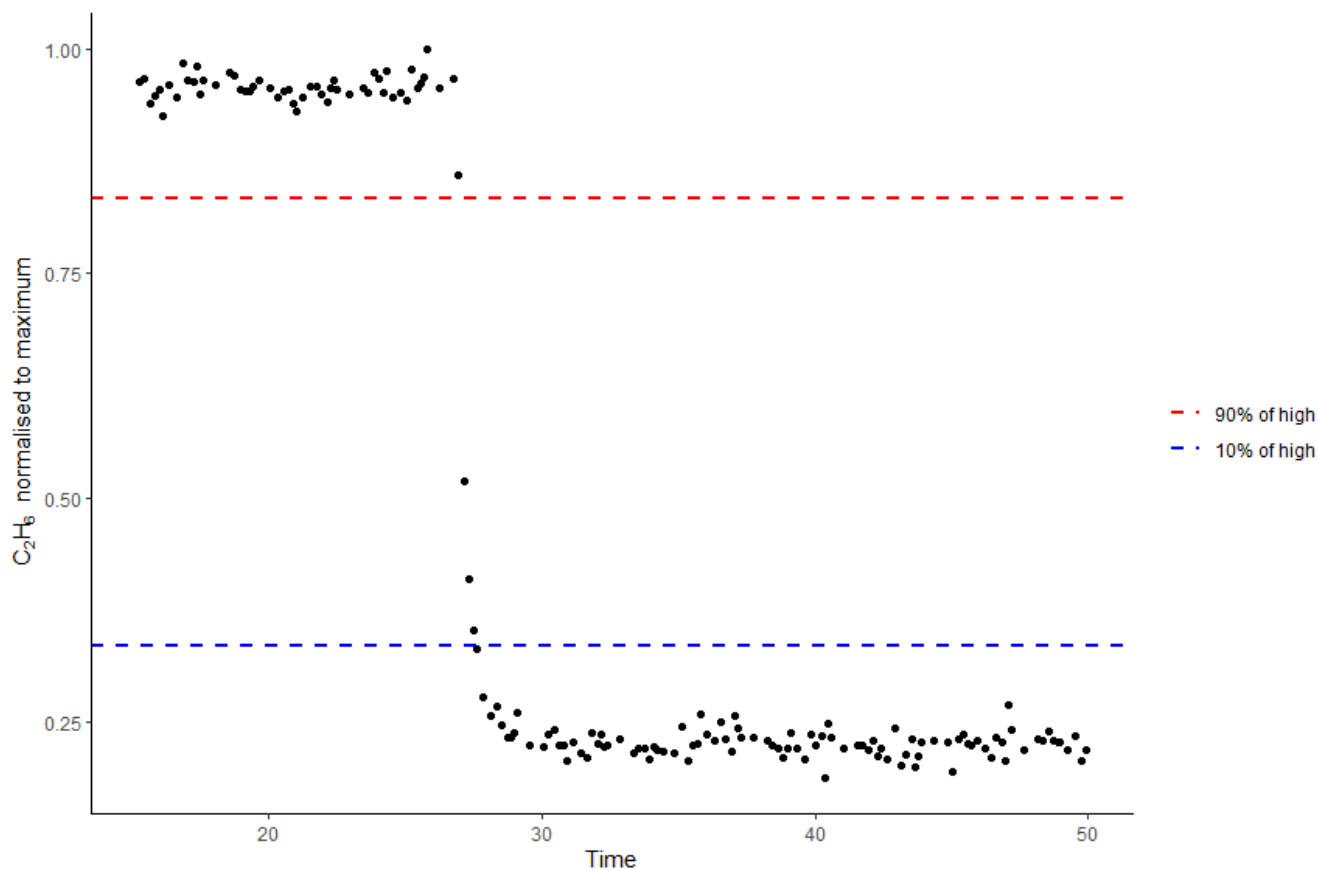
127 - m = Gradient of calibration concentration vs mean response averaged over the two calibrations

128 - c = Intercept of calibration concentration vs mean response averaged over the two calibrations

129 2.1.1 Instrument Response Time

130 Response time of the MGGA is reported as < 0.5 s from the manufacturer's specification. The response rate of the TILDAS
131 however was unknown. The TILDAS is capable of recording measurements at a rate of 10 Hz, however, the flow rate
132 through the instrument needed to be altered to make these measurements true to the 10 Hz values. Originally, the inlet to the
133 TILDAS had two valves in series, a ~~s~~Stainless ~~s~~Steel ~~i~~Integral ~~b~~Bonnet ~~n~~Needle ~~v~~Valve, 0.37 Cv, 1/4 in. #SS-1RS4 and an
134 electronic ~~u~~Upstream ~~f~~Flow ~~c~~Control ~~v~~Valve, 10,000 sccm, 0.25 in. ~~t~~Tube, ~~v~~Viton ~~s~~Seal #0248A-10000SV which allows
135 small changes to maintain the internal pressure at 70 Torr. With the two valves in series, the instrument ~~was~~is unable to
136 achieve a high enough flow rate for true 10 Hz measurements. Moving the valves to be parallel, the instrument was able to
137 achieve a flow rate close to 5 Hz, ~~at this point it was found that~~which indicated that the pump was the limiting factor for the
138 flow rate of the instrument.

139 These changes to increase the flow rate of the instrument were made to allow for a response time as close to that of the
140 MGGA as possible. To find the accurate response time of the TILDAS, an experiment was devised whereby a high
141 concentration of ~~C₂H₆ethane~~(17.630 \pm 0.715 ppb, measured via GC-MS) was flowed through the TILDAS and switched to
142 ambient air 10 times, on 2 separate valve setups, for a total of 20 repeats of low-high-low transitions in the concentration of
143 ~~C₂H₆ethane~~. The transition times were located by eye and then the transition time to go from 90_% of the maximum value to
144 10_% of the maximum value was calculated (*Symonds, 2017*), ~~a~~An example of the high to low transition with the 90 % and
145 10 % limits is shown in **Figure 1**. The transition time on the first valve ranged from 0.7 – 1.1 s with a mean value of 0.9 s,
146 the second valve had~~ving~~ responses ranging from 0.7 – 1.4 s, also with a mean response of 0.9 s, giving confidence in a sub
147 1 s response rate from the TILDAS and therefore showing the capability of a sub 1 s response in both instruments. The data
148 however was still averaged to 1 s with a 1 s clustering time due to the data ~~now~~being limited by the data acquisition rate of
149 the WASP's GPS.



151 *Figure 1: Example response transition of TILDAS high concentration to low concentration, normalised to maximum*
 152 *recorded response*
 153

154 2.1.2 Variation in methane measurements

155 Previous algorithms define an enhancement as being higher than 1.1 times a 2.5 minute rolling median background. This
 156 work however seeks to understand if this parameter holds true for the specific instrumentation used in the mobile surveys. To
 157 understand what this parameter may be, a variance experiment was undertaken. The standard deviation of ~~methane-CH₄~~
 158 measurements over this a 2 hour period was calculated to understand the minimum detectable enhancement for the
 159 ~~CH₄methane~~ detection algorithm.

160 For 2 hours compressed air was flown/flowes through the Los Gatos MGGA, with an observed measured at a median
 161 measured value of 7.2 ppm, ~~the and a~~ standard deviation of ~~these results was found to be~~ 0.006 ppm. An enhancement
 162 criteria was proposed as 5 times this standard deviation divided by the median baseline, resulting in an enhancement criteria
 163 of 1.005 times the baseline. However, this assumes a stable baseline that is replicated in the field. In reality, when applying

164 this enhancement criteria it ~~leds~~ to the detection of enhancements that ~~were~~ too small to be reliably quantified. Instead,
165 the ~~CH₄methane~~ mixing ratios measured during each mobile survey, were collated and the standard deviation was calculated
166 for each mobile survey. ~~Again~~ Enhancement criteria was calculated as anything larger than 5 times the standard deviation
167 divided by the median of ~~CH₄methane~~ mixing ratios. ~~†~~This was ~~done-repeated~~ for each mobile survey and resulted in a
168 median enhancement criteria of 1.01 times the baseline. However, as this ~~w~~ould result in detection of very small, diffuse, or
169 non-natural gas emission enhancements, enhancements that would be very small and could be diffuse or from enhancements
170 that occurred far from the roads and therefore harder to quantify as true natural gas emissions, a larger enhancement criteria
171 of 1.05 times the background was selected. This ensured there was still a large difference from the original methodologies
172 criteria, while still remaining within the instrumentation known variation.

173 2.2 Driving Route

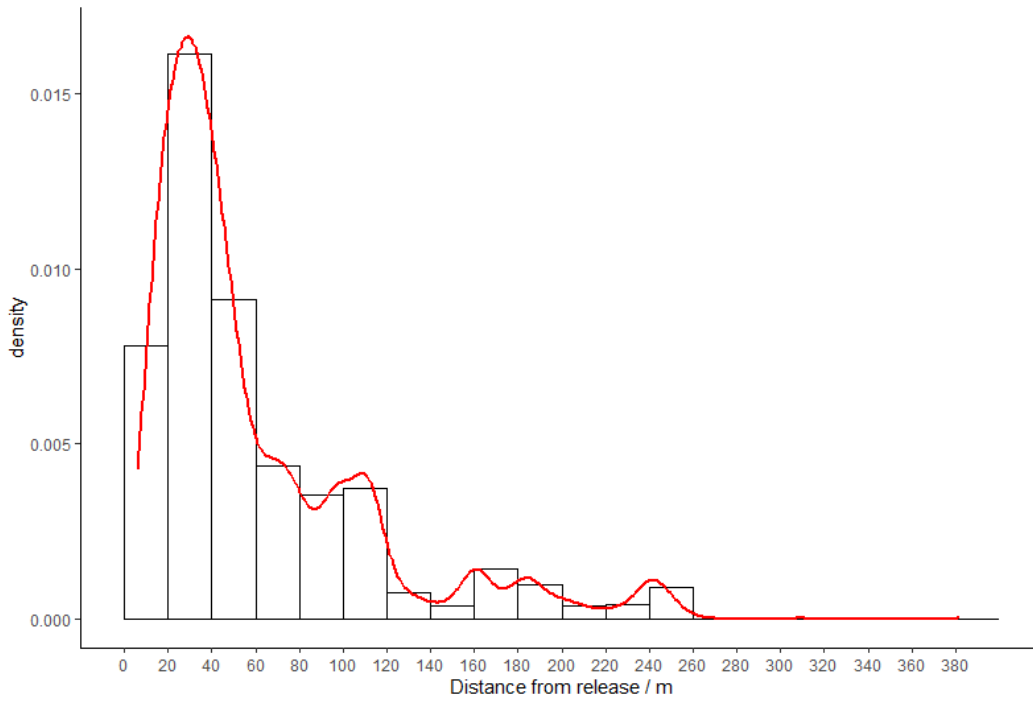
174 York is a city in the north-east of England with a population over 200,000. A driving campaign took place over two separate
175 weeks in May and June of 2024 resulting in 18 mobile surveys of a “flower petal” route, shown in **Figure 2**, staying within
176 the outer ring roads of the A64 and A1237 and mainly-focused primarily on sampling residential areas of the city. The
177 majority of the roads sampled on the route were only driven in one direction, but due to the position of the sampling inlet this
178 allowed the middle of the road to be sampled regardless of the direction of travel. The route was driven 18 times as, in order
179 to capture > 90 % of emissions, a route should be driven at least 5 - 8 times over separate days (*Luetschwager et al., 2021*).
180 The route was chosen as it covers multiple different neighbourhoods within York, but was not intended to be used to
181 compare measurements to the cities emissions inventory as it only covers a small fraction of the total miles of road within
182 the York urban area, 27 miles of a total 507 administered by the local authority (*Department for Transport, 2025*).

194 more than 110 % of the baseline, it must be 105 % of the baseline. This allows detection of smaller enhancements, ~~this~~
195 change was discussed in 2.1.2. LI determination occurred after identifying the source type of each OP, ensuring LI analysis
196 occurs only on OPs of the ~~same-thermogenic~~ source type, to further reduce the chance of comparing long standing
197 thermogenic fugitive emissions with possible nearby single occurrence pyrogenic or biogenic emissions.

198 2.4 Controlled Release Experiment

199 To ~~attain-obtain~~ a quantification equation specific to the equipment used ~~at~~in York, a controlled release experiment was
200 conducted at the Bedford Aerodrome. The controlled release took place at the Bedford Aerodrome over 5 days in ~~June-May~~
201 of 2024. A MiniCRF was deployed to manage releases of ~~CH₄ methane~~ and ammonia (~~NH₃~~), while a MidiCRF was deployed
202 for releases of ethane. In total, there were 41 releases lasting an average of 30 minutes each. Releases consisted of varying
203 amounts of ~~CH₄ methane~~ (0.2 - 70.48 L min⁻¹), ~~ethane-C₂H₆~~ (0 - 7.01 L min⁻¹) and ~~ammonia-NH₃~~ (0 - 7.87 L min⁻¹) to reflect
204 a range of methane sources, including natural gas and farm emissions. Releases were from a mixture of linear vertical
205 releases, a multi emission point ring, multi point source emissions and single point releases, occurring at heights ranging
206 from ground level to 3 m elevation. Over the course of the experiment wind speeds were measured using four Gill Met Pak
207 Pro instruments deployed at 3 m, 6 m, 9 m and 12 m elevation, winds were recorded as 1 minute vector averages. Average
208 wind speed over the 5 days was 3.87 m s⁻¹ with wind speeds ranging from 0 - 9.75 m s⁻¹. During each release, an initial
209 period was spent locating the plume before sampling the plume at set distances for 10 repeats, the platform then ~~stepped~~
210 ~~moved~~ further away in distance for another set of 10 repeats. ~~This~~ continued until the plume was either lost, or a lack of
211 driveable ground was left available. It was noted that larger releases were detectable further away, however, as the data from
212 the controlled release was intended to be used in quantifying under-road and near-road fugitive emissions of natural gas, a
213 maximum distance of 30 m ~~from the point of release was applied for data analysis to reflect the maximum from the~~
214 ~~controlled release point was applied, due to this reflecting the~~ maximum road widths typically found within a city like York
215 (*Essex Planning Officers Association, 2018*).

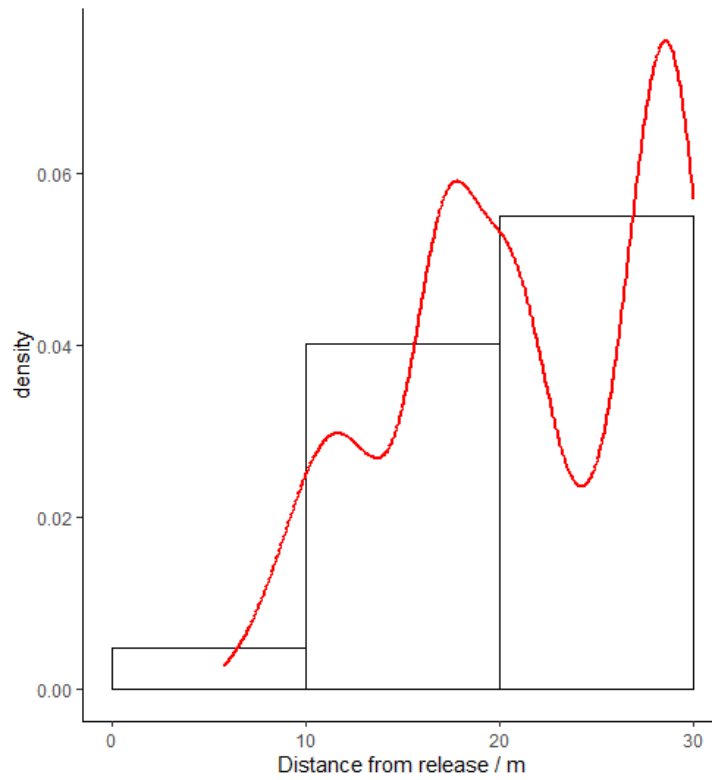
216
217 Of the 41 releases conducted in the controlled release, only 26 releases were able to be used for ~~processing data analysis, this~~
218 ~~is~~ due to several reasons, including ~~that~~ some releases ~~did~~ not have ~~ing~~ detectable enhancements. Within these 26 releases,
219 3525 ~~CH₄ methane~~ enhancements were detected over distances between 5.8 m and 382.1 m from the release point; the
220 majority of releases detected further away from the release point were from higher emission rate releases. When ~~this was~~
221 ~~enhancements were~~ filtered to ~~include enhancements up to~~ a maximum ~~distance~~ of 30 m from the release point, this resulted
222 in 1226 enhancements from 23 mobile ~~surveys~~ releases. Density plots of ~~the~~ number of detected enhancements against
223 distance from source are shown in *Figure 3* for all detected enhancements and *Figure 4* for enhancements detected within
224 30 m from the source.



225

226

Figure 3: Density plot of number of detected enhancements against distance from release point



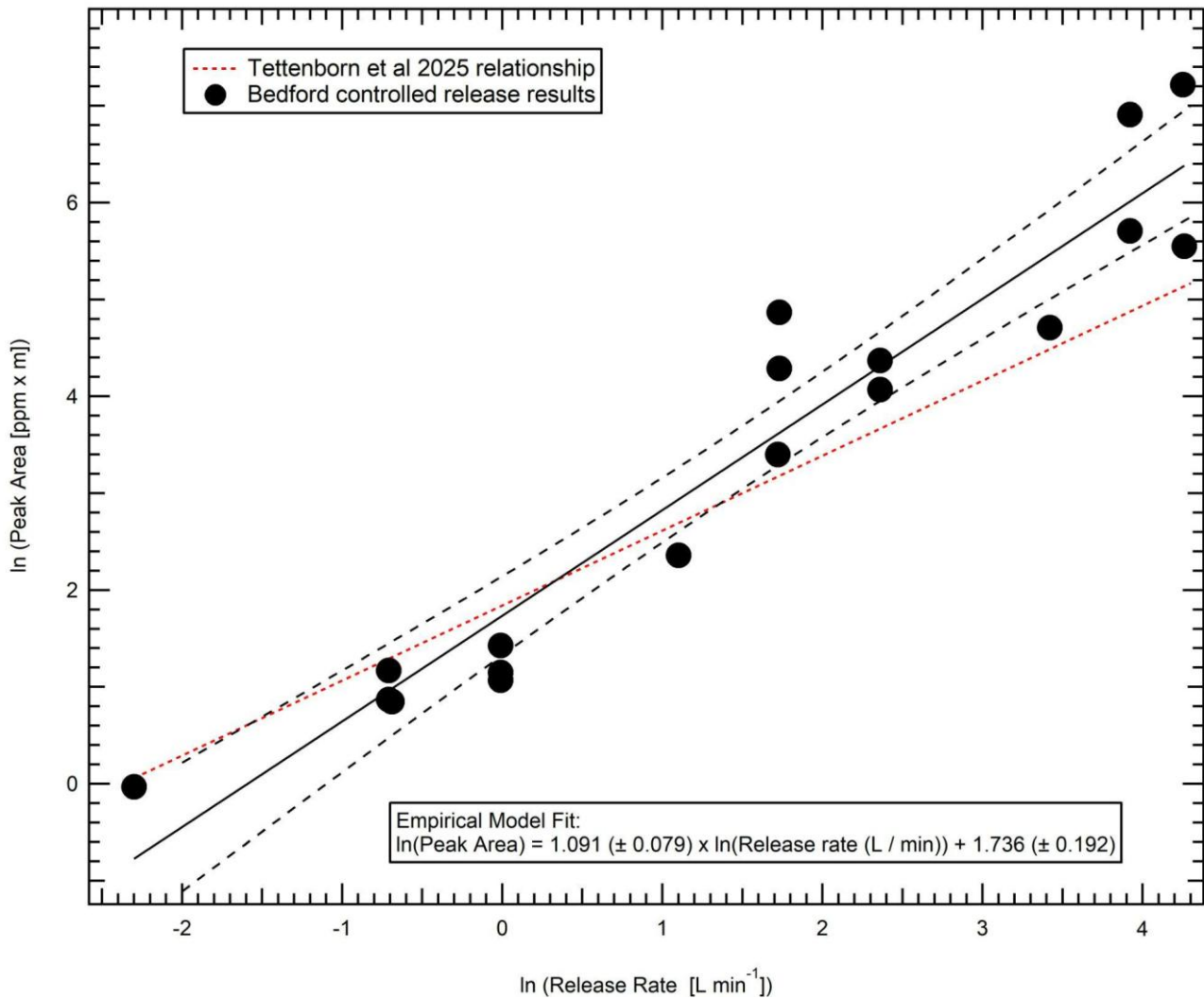
227

228 **Figure 4:** Density plot of number of detected enhancements against distance from release point (Limited to 0 – 30 m)

229 **2.4.1 Quantification equation**

230 There has been much development and advancement in the last few years on the use and application of “aAdvanced mMobile
231 Heak dDetection” systems for natural gas emissions detection and reporting. The original methodologies, where algorithms
232 were developed to convert peak height maxima of measured methane plumes to estimated emission rates (*Weller et al., 2019*)
233 have been superseded with plume area algorithms (*Tettenborn et al. 2025*) which are instrument and vehicle speed agnostic.
234 However, this is still not a precise conversion, and can only be treated as a generalised guide to emissions estimation as due to
235 external factors such as wind, instrument inlet location and local variability due to buildings and unknown source locations.
236

237 In order to reduce the uncertainty for the WASP as much as possible, we present the results of a 1-week controlled release
238 experiment conducted under variable wind conditions in a simple open field environment. Whilst this does not replicate the
239 complex conditions of an urban setting, previous work in (*Tettenborn et al. 2025*) shows that combined results from both urban
240 and open field settings can be combined to give a generalised trend to create their-a plume area emission algorithm. For the
241 WASP, the setup is slightly different to the work in (*Tettenborn et al. 2025*), with the WASP’s inlet located on the driver’s
242 side at low elevation. This may influence the impact of vehicle turbulence on the measurements and the difference in elevation
243 will lead to a different vertical section of the plume being sampled. A comparison between the results of the York-Bedford
244 controlled release, and the (*Tettenborn et al. 2025*) methodology averages are shown below in **Figure 5**. All data shown is for
245 downwind transects, where the plume was intercepted at a maximum of 30 m from the controlled release location. The plume
246 area is calculated as a function of distance travelled (as opposed to time), to correct for vehicle speed differences as done in
247 the original (*Tettenborn et al. 2025*) work.



248

249 **Figure 5:** Peak area vs actual release rate for plume transects within 30m of release. Data shown is an average of multiple
 250 transects (at least 10) for each release.

251

252 ~~As it can be seen in Figure 5, w~~Whilst the general trend of increasing plume area with release rate is adhered to, ~~as can be~~
 253 ~~seen in Figure 5,~~ the gradient of the trend is steeper, – implying that a near-ground based inlet is potentially more capable of
 254 ascribing differences in emission rates.

255

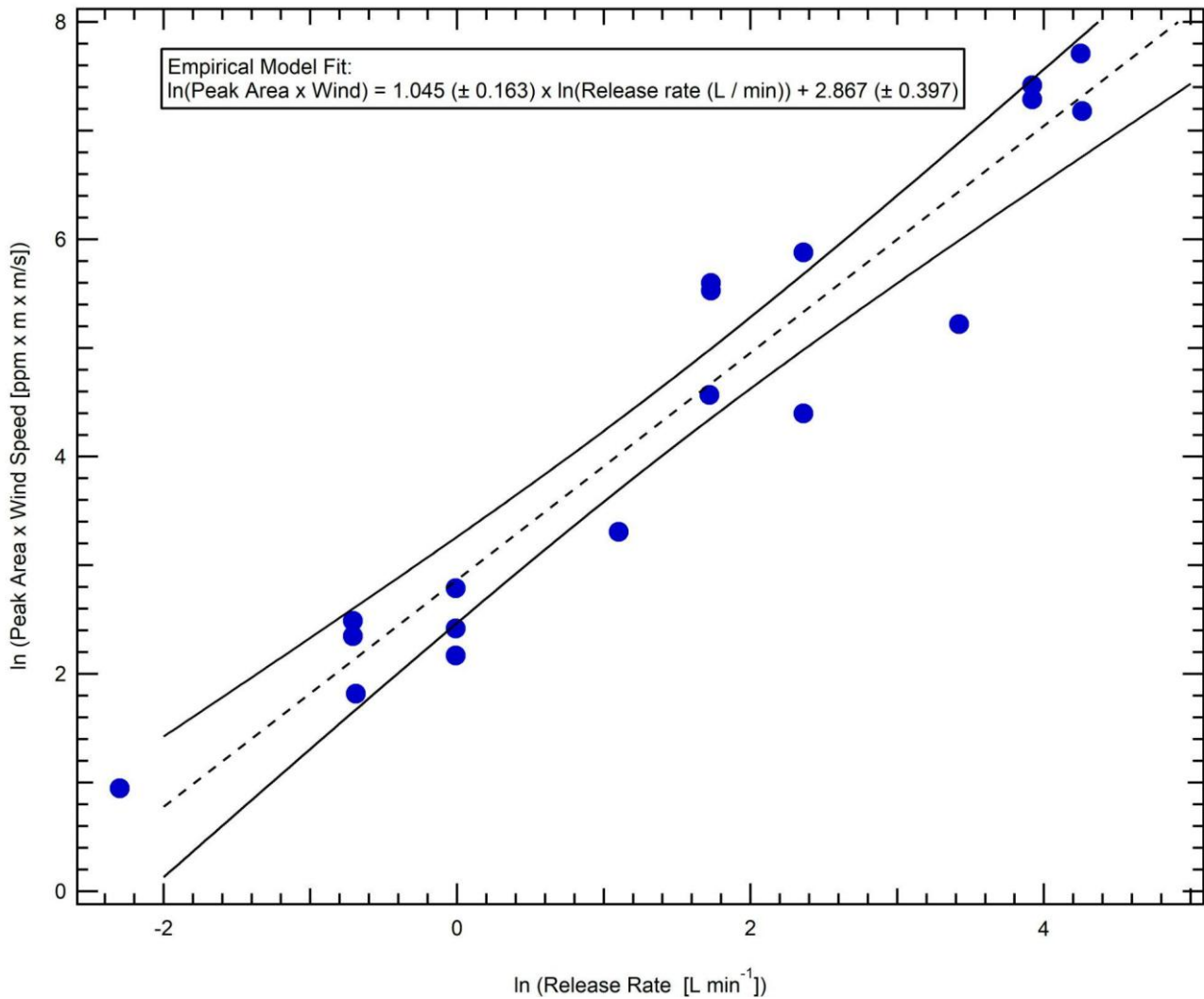
256 One of the expected limitations of these algorithmic methods is the assumption that the effect of windspeed is ignored, ~~–which~~
 257 ~~g~~Given the importance of windspeed in ~~more distal~~ emissions modelling

258 ~~(e.g. Gaussian plume modelling from vehicles (Dowd et al. 2024)), it would appear to have the potential for significant~~
259 ~~uncertainty in the resultant emissions quantification. To test this, 1 Hz wind data (averaged to 1 minute data) was taken from~~
260 ~~the 3 m mast located on site at the controlled release and incorporated into the analysis according to Equation 5.~~

261 ~~such as Gaussian plume modelling from vehicles (Dowd et al. 2024) may be an oversight. Using the 3 m mast, 1 Hz wind~~
262 ~~data (averaged to 1 minute data) located on site at the controlled release, the wind data is incorporated into the algorithm to~~
263 ~~give a volumetric correlation with the release rate according to Equation 5.~~

$$264 \quad \text{wind speed} \times \int_{\text{plume start}}^{\text{plume end}} [CH_4] \quad (\text{Eq. 5})$$

265 The results of the integration of ~~the~~ wind speed into the algorithm are shown below in **Figure 6**. Possibly somewhat
266 surprisingly, there is a slight decrease in the goodness of fit to the relationship, – potentially due to plume dynamics close to
267 source not being immediately controlled by the atmospheric conditions, but the dynamics of the emission. This may also
268 provide evidence as to the reasons why the results of previous studies have ended up with metrics that would at first ~~hand~~ seem
269 unlikely to be able to produce reliable results from atmospheric dispersion principles. Given this result, that it seems to be as
270 robust to consider wind as to not, it may be prudent for future controlled release experiments to focus on recreating the
271 conditions of gas migration prior to emission to the atmosphere to see if this result still holds true.



272

273 **Figure 6:** Peak area x Wind speed vs actual release rate for plume transects within 30m of release. As with Figure 5, data
 274 shown is an average of multiple transects (at least 10) for each release.

275

276 Due to these findings, the quantification equation used within York mobile surveys is shown in **Equation 6**.

277

$$\ln(\text{release rate} / \text{L min}^{-1}) = 0.9167 \times \ln(\text{Peak Area}) - 1.7359 \quad (\text{Eq. 6})$$

278

279 Additionally, leak rates were then reported within bins, similar to that within (Tettenborn et al., 2025), where three
 280 possible bins were assigned; high (> 40 L min⁻¹), medium (6 - 40 L min⁻¹) and small (< 6 L min⁻¹). This was adapted
 281 for the York surveys, the small category was changed to 2 - 6 L min⁻¹ and a new category, very small, was introduced

282 which contained leak rates of 0 - 2 L min⁻¹. This change was introduced due to the lower enhancement criteria within
283 the York methodology ~~allowed which allows~~ for detection of much smaller fugitive emissions.

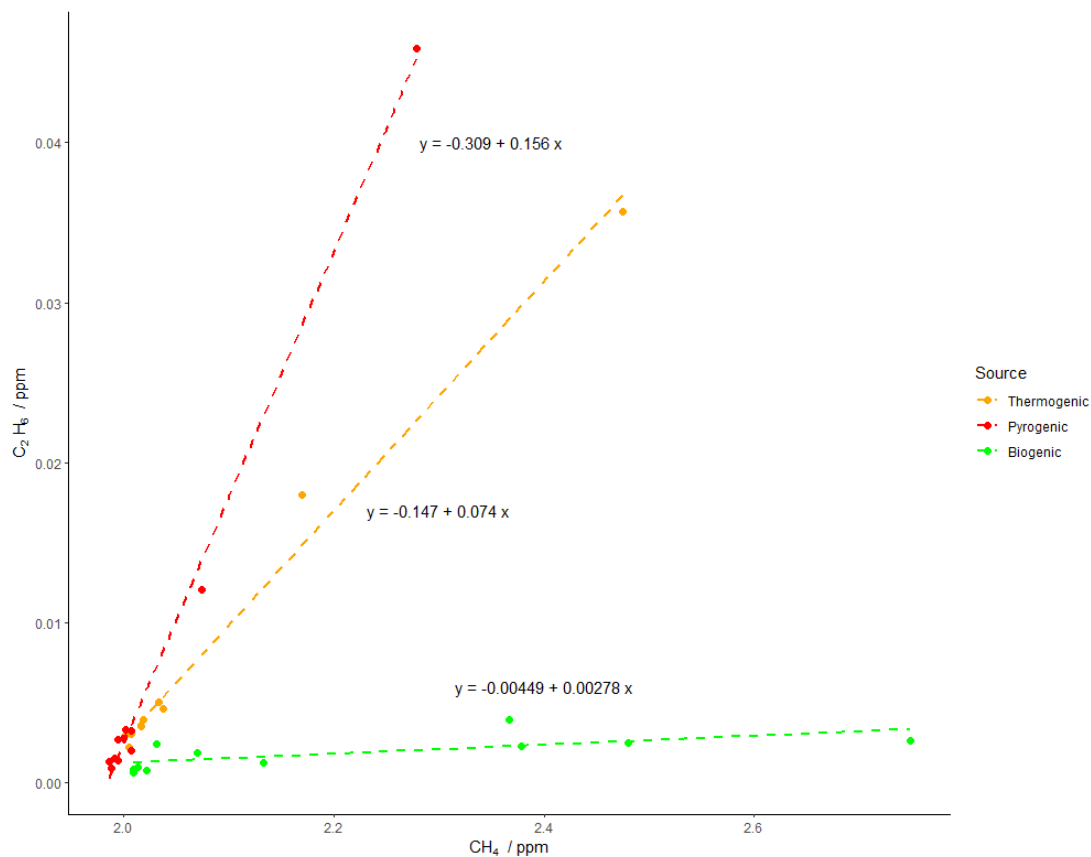
284
285 It is important to note that these results are only suitable for the specific set-up utilised here, and should not be more widely
286 applied without corroboration with other instruments or platform packages.

287 2.4.2 Instrument Lag Time

288 For each of the releases, the lag time between detecting an ~~ethane-C₂H₆~~ enhancement and a ~~CH₄methane~~ enhancement was
289 calculated. Due to the response times of the instruments, it was expected that the TILDAS would respond to an enhancement
290 before the MGGA, however, this assumes that both instruments receive the same packet of air at the same time, while, in
291 reality, the packet of air will take a different amount of time to flow through ~~the~~ manifold to each instrument. To ~~find this~~
292 ~~determine a~~ more accurate lag time ~~of for~~ the instruments, the maximum ~~CH₄methane~~ enhancement for each ~~transect~~ pass was
293 ~~found, following this identified along with~~ the maximum ~~C₂H₆ethane~~ enhancement ~~was found (that occurred within 5 seconds~~
294 ~~of the methane) occurring within 5 seconds of the CH₄ enhancement~~. The resulting 10 second window was selected ~~as based~~
295 ~~on transects of the vehicle speeds during the~~ controlled release, ~~where~~ the ~~van WASP~~ travelled at roughly 20 miles hour⁻¹.
296 Over the course of 10 s (5 s either side of the methane maximum) this would ~~mean result in a distance of~~ 85 m covered ~~in the~~
297 ~~van,~~ (the average length of a transect being 180 m). The time lag between ~~C₂H₆ethane~~ and ~~CH₄methane~~ showed that in most
298 cases (88.1 %), maximum ~~C₂H₆ethane~~ concentration preceded maximum ~~CH₄methane~~ concentration with a mean ~~lag~~ of 2.7 s
299 before and a median of 3.8 s before. Observing a window of ~~time of maximum CH₄ methane~~ to 5 s before maximum
300 ~~CH₄methane~~ resulted in a mean lag of 3.3 s from ~~C₂H₆ethane~~ to ~~CH₄methane~~ and a median lag of 3.9 s. This helped inform
301 the detection algorithm to look for maximum ~~C₂H₆ethane~~ within a window only up to 5 s before the maximum ~~CH₄methane~~.
302 Density plots showing the time lag of maximum ~~C₂H₆ethane~~ from maximum ~~CH₄methane~~ are shown in *Figure S2* for the full
303 10 second time window and *Figure S3* for up to 5 seconds before the time of maximum measured ~~CH₄methane~~.

304 2.5 Source Apportionment

305 Source determination using ethane ~~:~~ methane (~~C₂:C₁~~) ratios has been shown to be effective, due in part to the knowledge that
306 ~~C₂H₆ethane~~ is present in measurable quantities in thermogenic gas but not biogenic gas (*Fernandez et al., 2022*). ~~These~~
307 ~~ethane:methane (C₂:C₁)~~ ratios can be used in order to determine the source of a ~~CH₄methane~~ emission. Demonstrated in
308 (*Yacovitch et al., 2014; Lowry et al., 2020; Defratyka et al., 2021; Fernandez et al., 2022*), C₂:C₁ < 0.005 may be associated
309 with biogenic sources, > 0.005 to < 0.09 are thermogenic and > 0.1 are considered pyrogenic or combustion. Ideal examples
310 of these relationships are shown in *Figure 7*. In order to calculate these ratios ~~CH₄methane~~ and ~~C₂H₆ethane~~ values must first
311 be aligned in time, due to them being measured on separate instruments, the criterion for time alignment was discussed in
312 **2.4.2**. Additionally, enhancements are removed where the R² of CO₂:CH₄ is greater than 0.9 to ensure no combustion sources
313 are wrongly assigned as thermogenic.



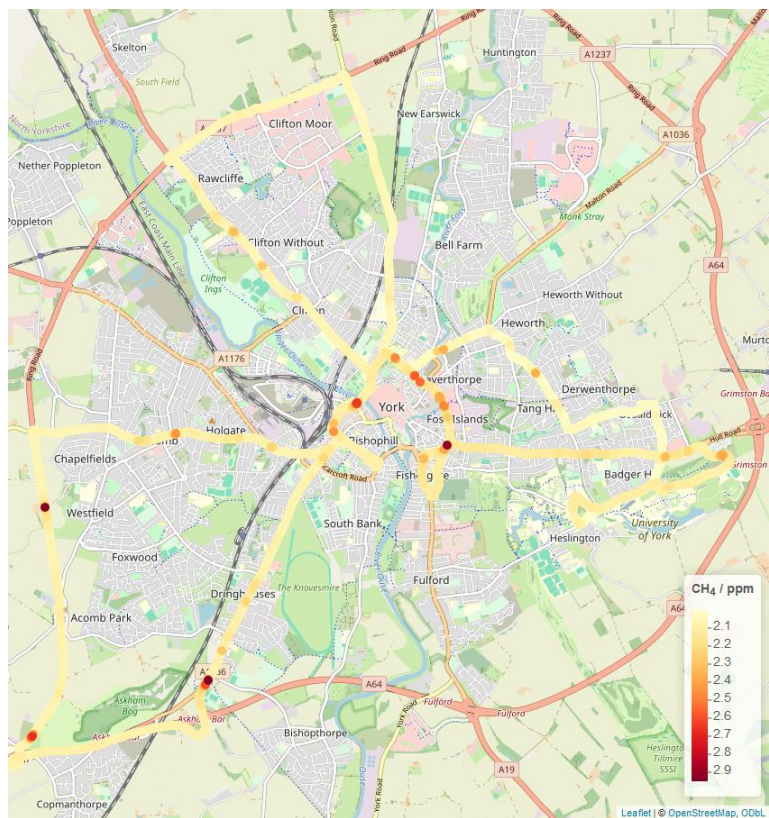
314
 315 **Figure 7:** Relationship between CH₄ and C₂H₆ for three OPs of different source types located during the sampling
 316 campaign.

317 **3 Results**

318 **3.1 Results of York mobile surveys**

319 17 mobile surveys were conducted across the route of York, the raw data was taken from 10 Hz files for CH₄ methane
 320 (MGGGA) and C₂H₆ ethane (TILDAS) and time averaged to 1 Hz data to be of the same response time as the WASPs other
 321 internal components (e.g. GPS), a colour map of the resulting measured CH₄ methane concentration is shown in **Figure 8**.
 322 The data was then processed to remove data measurements taken when vehicle speeds were 0 or > 40 miles hour⁻¹ as well as
 323 removing data within the area of Wolfson Atmospheric Chemistry Laboratories WACL, due to this also being the location
 324 within which calibrations and other instrument tests were conducted in this location. A rolling 2.5-minute median
 325 background of CH₄ was then applied and enhancements were determined as any CH₄ measurement taken that was greater
 326 than 1.05 times the calculated background. The enhanced readings were then clustered such that any elevated reading within

327 one second of another were assumed to correspond to the same enhancement. These enhancements were then spatially
328 averaged such that 468 OPs were detected over the course of the 18 mobile surveys.
329



330
331 **Figure 8:** Colour map of CH₄ concentration from one of the York mobile surveys.
332

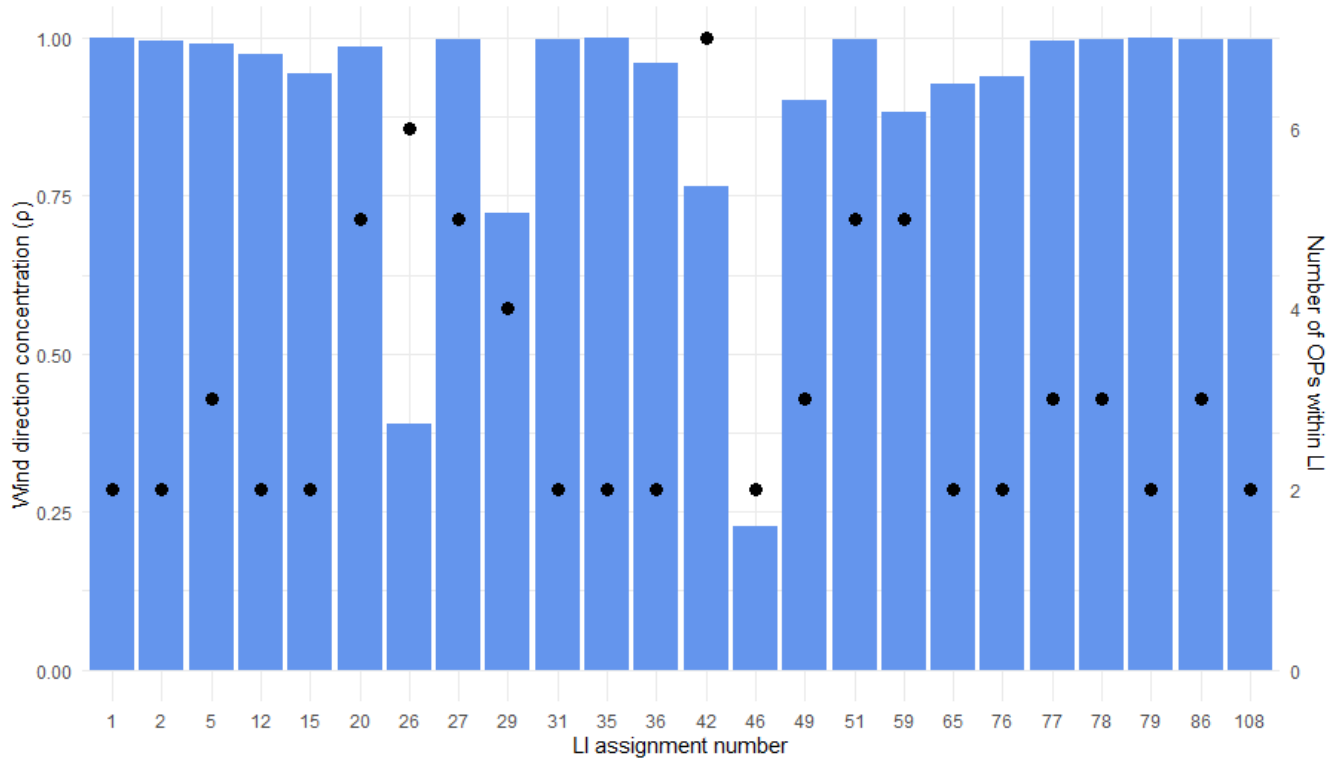
333 For each of these OPs the maximum C₂H₆ ethane-value was found from the time of maximum CH₄ methane to 5 seconds prior.
334 The two instruments' data were then aligned for each OP such that time of maximum CH₄ methane-measurement was equal to
335 time of maximum C₂H₆ ethane measurement. A linear regression was then taken of values from 5 seconds prior to the maximum
336 CH₄ methane measurement to 5 seconds after and a source type was assigned such that C₂:C₁ < 0.005 is associated with biogenic
337 sources, > 0.005 to < 0.09 are thermogenic and > 0.1 are considered pyrogenic or combustion.

338
339 This meant that of the 468 OPs, 177 (37.8 %) were found to be thermogenic in origin. Each AllF thermogenic OP was reas
340 then spatially clustered using a 30 m threshold, with the resulting clusters to find others within 30 m of one another and filtered
341 to ensure that each clusters contained OPs occurring on at least two separate mobile surveys, to remove any OPs occurring
342 from an event happening-observed on during only one mobile survey. The remaining clusters were then averaged into LIs such
343 that the latitude and longitude were calculated as a weighted spatial average, resulting in 24 thermogenic LIs from the 177

344 thermogenic OPs. Leak rate was determined using the equation present in 2.4.1 using the mean $\ln(\text{peak area})$ of all OPs within
 345 ~~the each~~ LI cluster. The smallest leak rate was determined to be 0.01 L min^{-1} and the largest being 4.13 L min^{-1} , when assigned
 346 to bins 2 were ~~classified as~~ small ($2 - 6 \text{ L min}^{-1}$) and 22 were very small ($0 - 2 \text{ L min}^{-1}$). When the source ~~type filter determination~~
 347 ~~step is was~~ omitted, ~~this it resulted~~ in 58 LIs with leak rates ranging from 0.01 to 4.70 L min^{-1} , when assigned to bins 9 were
 348 small ($2 - 6 \text{ L min}^{-1}$) and 49 were very small ($0 - 2 \text{ L min}^{-1}$).

349 3.1.1 Industry applicability

350 As many gas distribution companies have signed up to voluntary emission reporting programmes, such as the Oil and Gas
 351 Methane Partnership (OGMP) 2.0, they are now obligated to report emissions through measurement based methods. One of
 352 the most popular methods for such a reporting programme is through comprehensive, repeated vehicle based measurement
 353 surveys of an operator's gas network. Here, we have a repeated route of measurements where thermogenic emissions have
 354 been reported at certain locations throughout the campaign. It is therefore interesting from a mitigation perspective to
 355 investigate how many times each ~~of those~~ thermogenic emissions ~~was ere identified detected~~ over the course of the campaign.



356
 357 **Figure 9: Wind direction consistency and number of OPs per thermogenic leak indication**
 358

359 The effect of wind on detection of LIs was initially investigated by calculating the mean resultant length of wind directions
 360 when a thermogenic OP was detected. This was calculated using Equation 7.

361

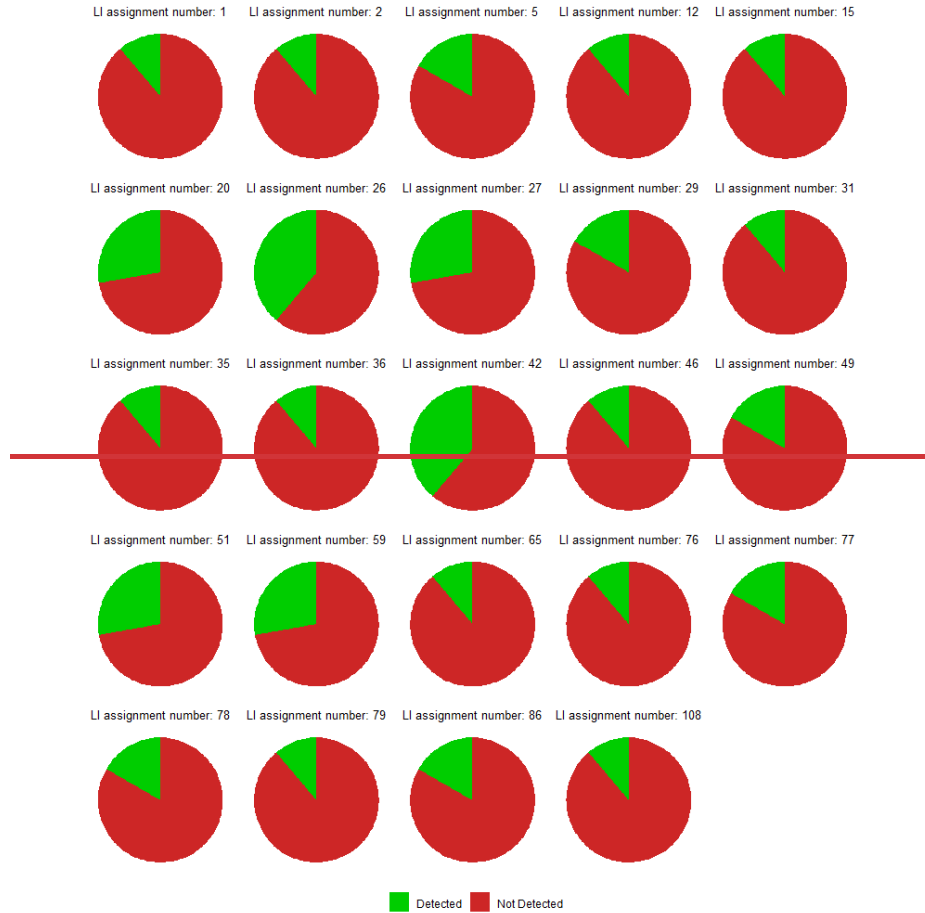
$$\rho = \frac{1}{n} \sqrt{(\sum_{i=1}^n \cos\theta_i)^2 + (\sum_{i=1}^n \sin\theta_i)^2} \quad (\text{Eq. 7})$$

362 Where:

- 363 - ρ is mean resultant length
- 364 - n is number of data points
- 365 - θ_i is the angle in radians

366 For this analysis ρ is close to 1 when the wind directions are concentrated (similar) and close to 0 when more dispersed.

367 **Figure 9** shows that for the majority of LIs detected in York, ρ is close to 1, suggesting that most LIs occur away from the
 368 road and require correct wind direction ~~in order to detect them~~ to be detected.



369

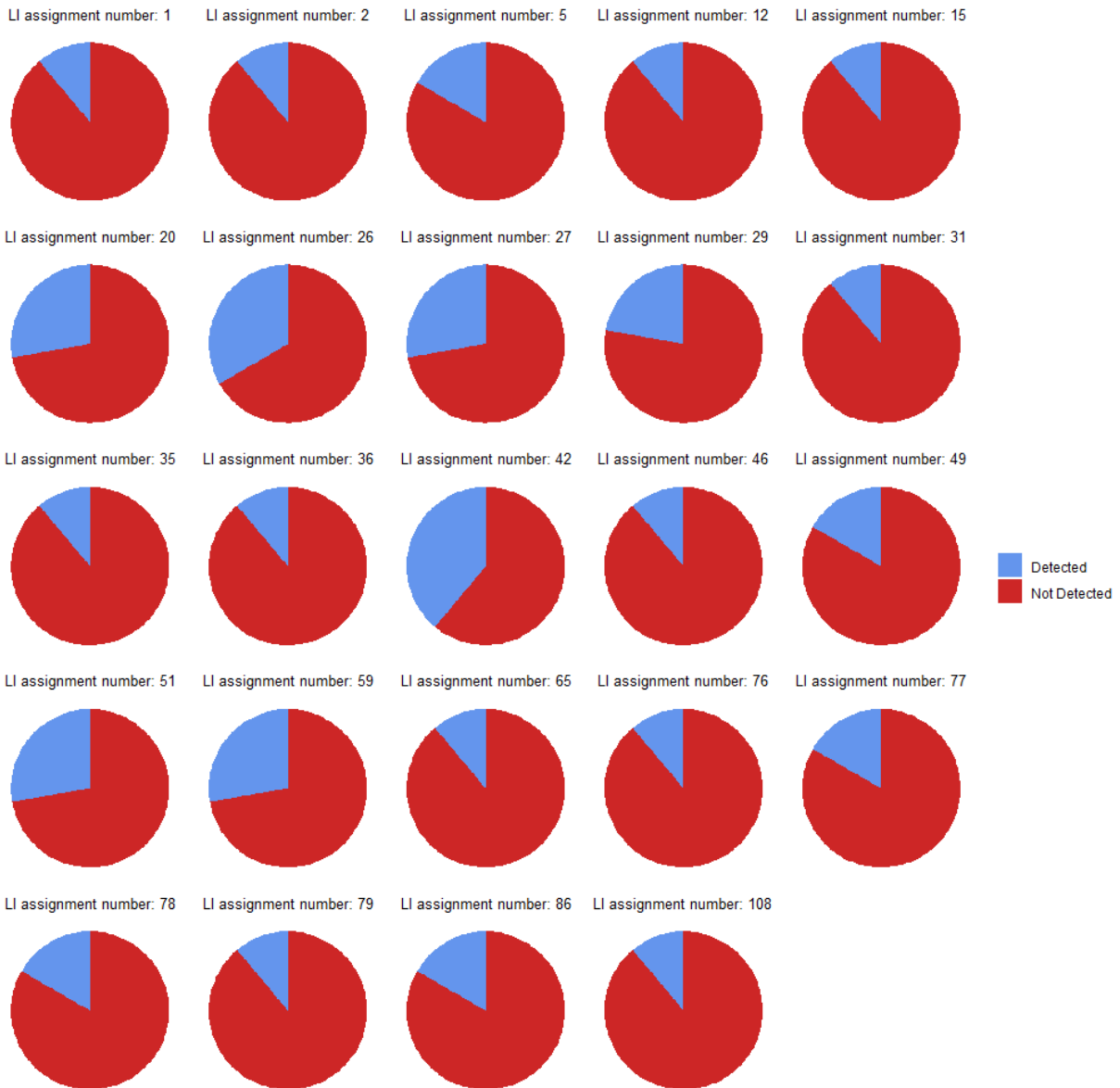


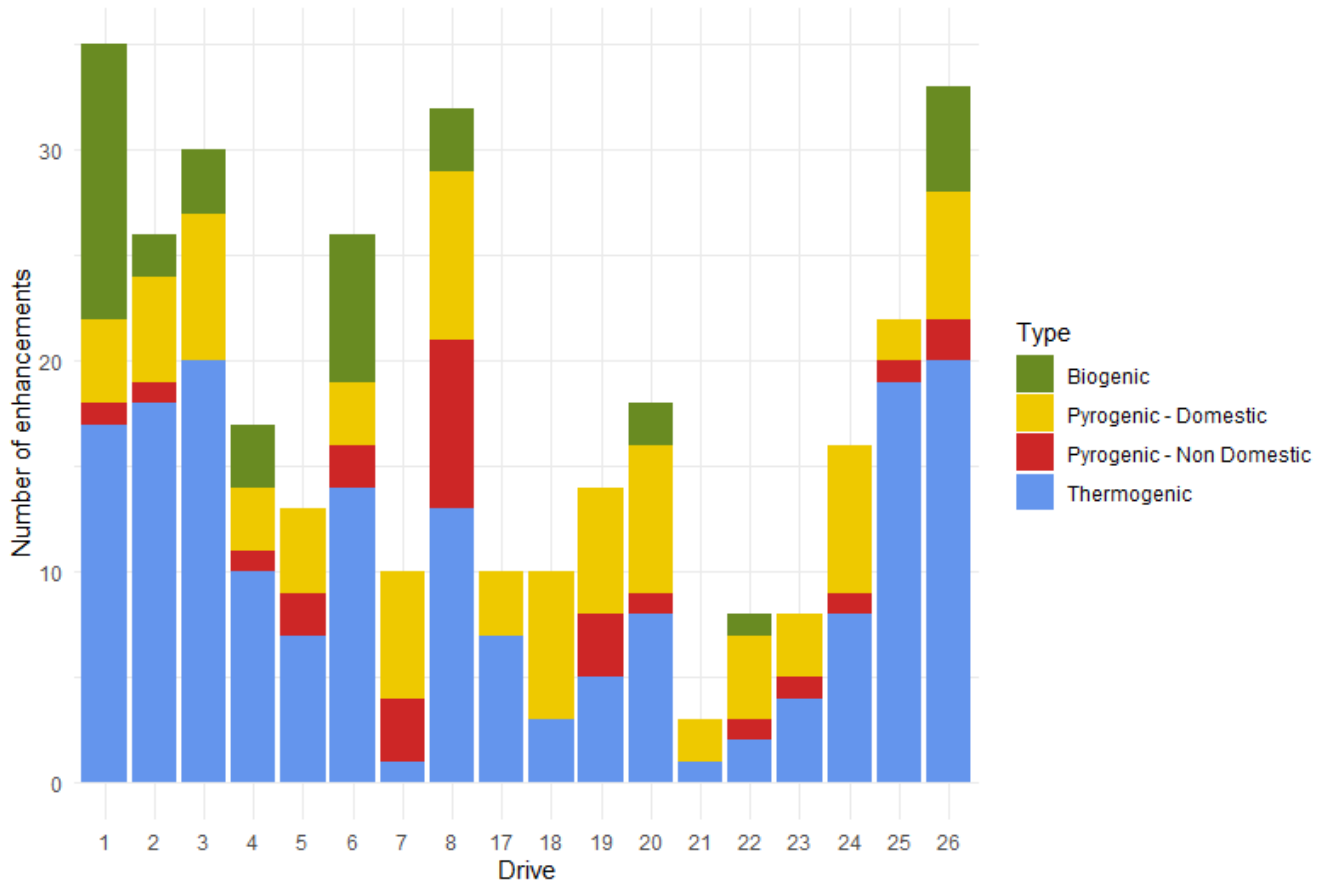
Figure 10: Pie charts of each LI showing number of mobile surveys they were detected vs not detection frequency.

The number of mobile surveys is a large factor in the probability of detecting an LI. Each LI requires the enhancement to be detected on at least 2 separate mobile surveys, for the. Of the 24 LIs detected over the course of this campaign, 12 LIs were detected on 2 mobile surveys, 6 were detected on 3 mobile surveys, 4 on 5 mobile surveys and 2 on 7, this meant that the resulting in an average probability of detection was of 0.18. Detection versus non detection for each LI is demonstrated in **Figure 10**. This low probability of detection highlights the need for surveys with multiple passesrepeats.

378 **3.2 Emissions from other sources**

379 While 177 of the 468 OPs were determined to be thermogenic, 39 were assigned as biogenic (8.3 %), 199 were pyrogenic
380 (41.8 %) and 53 were not able to be assigned a source type. NO_x:CO₂ ratios were investigated for the pyrogenic OPs using the
381 same methodology used for the CH₄:C₂H₆:C₂:C₁ source assignment. 115 of the 199 pyrogenic OPs were able to be analysed
382 in this way, 87 of these 115 OPs (75.7 %) had a NO_x:CO₂ ratio < 0.88 x 10⁻³. This implied that the majority of pyrogenic
383 emissions did not originate from traffic, but were more likely emissions from domestic heat and power generation (such as
384 emissions from domestic boilers) (Cliff *et al.*, 2025).

385 Emissions from pyrogenic and biogenic sources are-were compared to thermogenic source-emissions at the OP stage on a
386 mobile survey by mobile survey basis due to the high unlikelihood of pyrogenics and biogenics being persistent emission
387 sources, the number of times each source type was detected per mobile survey is shown in *Figure 11*.



388
389 *Figure 11: Total number of enhancements from each source type for each of the mobile surveys.*

390
391 Thermogenics were the most frequently located source type on 13 of the 18 surveys, with mobile surveys 7, 18, 19, 21 and
392 22, finding pyrogenic emissions related to heating and cooking were the most frequently occurring source type.

393 **3.3 Comparison to previous methods**

394 The main alterations to this methodology from that presented in (Weller *et al.*, 2019) (and other studies that were based off
 395 this method) ~~were that was the decrease in~~ enhancement criteria ~~was changed~~ from 1.1 times the baseline to 1.05 times the
 396 baseline, ~~a decrease in the clustering time window from 5 s to 1 s~~ ~~clustering by time was changed such that emissions within~~
 397 ~~1 s of each other were clustered instead of those within 5 s. Finally and the addition of~~ a source determination stage ~~was~~
 398 ~~added~~ as a core step in the algorithm, as opposed to previous iterations that either had no source determination stage or one
 399 that came later in the analysis. ~~Table 1 shows~~ *Table 1* shows the effect ~~that all of each~~ of these changes ~~to the methodology make~~
 400 on the resulting detection of OPs and LIs.
 401

Enhancement Criteria	Time Clustering Criteria / s	Source Determination Included?	Number of OPs	Number of LIs
110% of baseline	5	No	179	27
		Yes	66	6
	1	No	216	29
		Yes	79	7
105% of baseline	5	No	357	58
		Yes	144	23
	1	No	468	58
		Yes	177	24

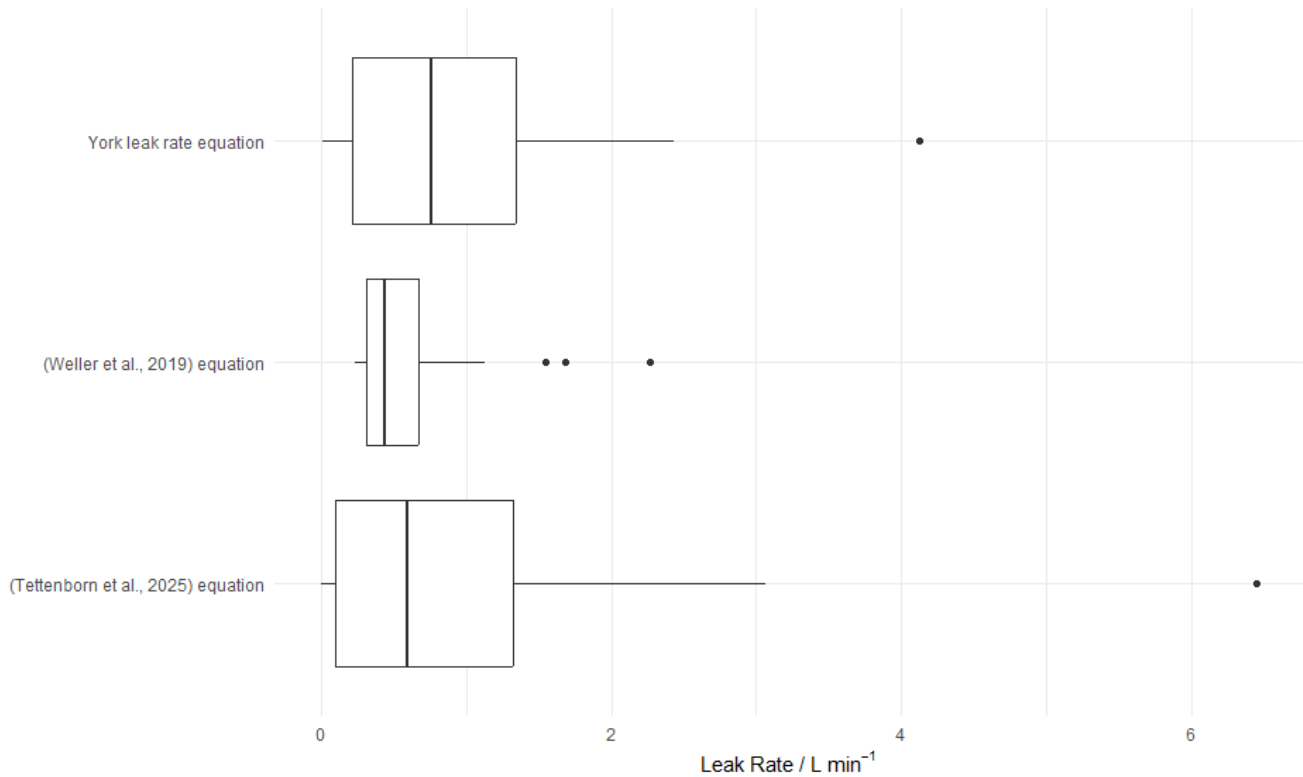
402 *Table 1: Number of detected OPs and LIs depending on ~~changing~~ algorithm parameters*

403
 404 ~~This shows~~ *These results show* -the new methodology could locate more LIs. Binning into the leak rate categories of very
 405 small (0 - 2 L min⁻¹), small (2 - 6 L min⁻¹), medium (6 - 40 L min⁻¹) and high (> 40 L min⁻¹) showed that of the 24 LIs in the
 406 new source filtered methodology, 2 were small and 22 were very small. For the 58 LIs of the new non filtered methodology,
 407 9 were small and 49 were very small. ~~For For the~~ 27 LIs ~~from the old non filtered detected in the original unaltered~~
 408 methodology 10 were small and 17 were very small. Finally, ~~for~~ the 6 LIs ~~detected when applying the source determination~~
 409 ~~step to the original unaltered methodology, from the old source filtered methodology,~~ 1 was small and 5 were very small.
 410 This shows the ~~original old~~ methodology, requiring an enhancement of 1.1 times the baseline with 5 s time clustering, misses
 411 a large proportion of LIs that the newer methodology, requiring an enhancement of 1.05 times the baseline with 1 s time
 412 clustering, detects. A large proportion of these missed LIs occur in the very small category as expected with a smaller
 413 enhancement criteria. Source filtering shows that regardless of criteria used, less LIs will be detected with this ~~included in~~

414 ~~the method.~~ This suggests previous methodologies that do not use this stage may be mischaracterising some thermogenic
415 enhancements as being permanent, as they may instead be detecting methane enhancements of differing source types that
416 occur within the same vicinity of one another.

417 3.4 Comparison of alternate quantification approaches

418 As previously described, the quantification equation used within this body of work is based on the (Tettenborn et al., 2025)
419 approach of using peak area to calculate the leak rate of a LIs. However, previous works have used the quantification equation
420 present in (Weller et al., 2019) which ~~instead~~ quantifies release rate based on peak height. This campaign's results were
421 reprocessed using each of these previous quantification equations in order to compare the effects of the updated parameters in
422 the York quantification equation to the original, present in (Tettenborn et al., 2025) but also to explore the difference in
423 quantified leak rates from a peak height approach. As previously mentioned, the results of the York quantification approach
424 resulted in the 24 LIs being assigned to leak rate bins such that 2 were small and 22 were very small, the (Tettenborn et al.,
425 2025) equation results in 1 medium, 1 small and 22 very small and the (Weller et al., 2019) equation results in 1 small and 23
426 very small. The specific leak rates of LIs calculated with these three equations are presented in box-plots in **Figure 12**.



427 **Figure 12:** Comparison of calculated leak rates of LIs from each of the 3 quantification equations.
428
429

430 This shows that both the peak area approaches result in a much larger range of calculated leak rates from the LIs than from the
431 peak height approach present in (Weller et al., 2019). This suggests that the instrumentation used to detect CH₄ enhancements,
432 may result in low, wide peaks as opposed to higher, sharper peaks, thus explaining why leak rates are weighted much lower
433 from this method. The (Tettenborn et al., 2025) equation appears to be mostly consistent with the equation determined from
434 the York methodology, however there is slightly higher weighting of leak rates with the (Tettenborn et al., 2025) equation,
435 resulting in the 24 LIs changing from the assignments of 5 small and 19 to 1 medium, 5 small and 18 very small.

436 4. Conclusions

437 This study focused on using the limitations of ~~surveying~~ instrumentation to better inform a detection algorithm.
438 Enhancement criteria was determined by investigating the variance of the MGGA, although laboratory experiments
439 suggested the instrumentation was capable of detecting enhancements at a minimum of 1.005 times the baseline was
440 possible, in-field experiments showed that ~~an~~ enhancement criteria of 1.01 times the baseline was more likely the lower
441 limit for detection. However, for the surveys a criteria of 1.05 ~~times the background~~ was selected so as to not incorporate
442 small, diffuse emissions within the analysis. Response rate of the instruments was calculated to inform the time window for
443 clustering, with both MGGA and TILDAS having sub ~~one-second-1 s~~ response rate, the time clustering was ~~instead~~ limited
444 to ~~one-second-1 s~~ due to the limitations of GPS data collection speed. ~~Employing the parameters used in previous~~
445 ~~methodologies, resulted in the~~ ~~These changes show previous methodologies would result in~~ detection of 27 LIs compared to
446 the 58 LIs ~~detected~~ using updated parameters (53.5 % less), the parameter change has also shown the ability to detect more
447 LIs in all leak rate categories, but in particular, the very small (0 - 2 L min⁻¹) category, where 17 of 27 LIs were located in
448 the previous methodology, but 46 of the 58 were located in the new methodology.

449 Source ~~appointment-determination~~ proved to be a useful tool for predicting emissions directly related to natural gas, when
450 source filtering was introduced at the OP stage of detection, it resulted in only 41.4 % of LIs still being detected as opposed
451 to the non-source filtered method.

452 Additionally, source ~~filtering-determination~~ has helped to highlight that although ~~t~~ thermogenic emissions from natural gas
453 are the highest contributor to ~~CH₄ methane~~ emissions, pyrogenic emissions related to domestic heat and power generation
454 also provide a high, but often overlooked contribution to a city's ~~CH₄ methane~~ emissions.

455 ~~The~~ ~~U~~ ~~pp~~ ~~dat~~ ~~ing~~ ~~of~~ the quantification equation from a peak height approach to a peak area approach ~~result~~ ~~eds~~ in a much wider
456 range of leak rates being calculated in the study. ~~H~~ ~~h~~ ~~ow~~ ~~ever~~, these values ~~are~~ ~~were~~ not as high as when quantified using the
457 original equation presented in (Tettenborn et al., 2025).

458 This new method has shown that ~~with~~ ~~by~~ changing enhancement criteria and time clustering parameters, it is ~~able~~ ~~possible~~ to
459 detect many more LIs, ~~and~~ ~~but~~ that by applying a source ~~type~~ ~~filter~~ ~~determination~~ ~~step~~ at the OP detection stage ~~there is a~~
460 ~~reduction in the number of detected LIs due to the reduction~~ ~~it is capable of reducing~~ the incorrect assignment of ~~LIs~~ ~~OPs~~.
461 However, the methodology has ability to improve further, primarily by ~~using~~ ~~employing~~ instrumentation that is capable of

462 detecting ~~both CH₄ methane and C₂H₆ ethane on one instrument~~, so as to remove uncertainty related to time lag between ~~the~~
463 two instruments, ~~but s~~Secondly, improvement can be made by having all instrumentation and hardware able to operate at a
464 sub ~~one-second-1 s time-response~~ rate in order to reduce the time clustering parameter limit and further improve spatial
465 resolution.

466 **Code / Data availability**

467 Code and data will be made available upon request.

468 **Author Contribution**

469 Contributed to conception: TM, JH, WD, JL. Contributed to data acquisition: TM, JH, WD, SY, SHB, MS, JL. Contributed to
470 analysis and interpretation of data: TM, JH, WD, SY, JF, JL. Initial draft of paper: TM. Subsequent drafts and/or revisions to
471 paper: TM, JH, WD, SY, DL, JF, JL. Approved the submitted version of this paper for publication: TM, JH, WD, SY, SHB,
472 MS, JF, DL, JL.

473 **Competing Interests**

474 The authors declare that they have no conflict of interest.

475 **Acknowledgements**

476 We would like to thank the INGENIOUS (Understanding the sourceS, traNsformations and fates of IndOor air pollUtantS)
477 project, NERC grant number NE/W002256/1, for providing access to their data in the early stages of the method development.
478 Additionally we would like to thank both the National Physical Laboratory (NPL) and the MOMENTUM (Mobile
479 Observations and quantification of Methane Emissions to inform National Targeting, Upscaling and Mitigation) project, NERC
480 grant number NE/X014649/1, for organising and providing access to the controlled release experiment.

481 **References**

482 Ars, S., Vogel, F., Arrowsmith, C., Heerah, S., Knuckey, E., Lavoie, J., Lee, C., Pak, N.M., Phillips, J.L. and Wunch, D.,
483 Investigation of the spatial distribution of methane sources in the greater Toronto area using mobile gas monitoring systems.
484 Environ. Sci. Technol., 54(24), pp.15671-15679. <https://doi.org/10.1021/acs.est.0c05386>, 2020.

485

486 Bačėninaitė, D., Džermeikaitė, K. and Antanaitis, R., Global warming and dairy cattle: How to control and reduce methane
487 emission. *Animals*, 12(19), p.2687. <https://doi.org/10.3390/ani12192687>, 2022.

488

489 Chamberlain, S.D., Ingrassia, A.R. and Sparks, J.P., Sourcing methane and carbon dioxide emissions from a small city:
490 Influence of natural gas leakage and combustion. *Environ. Pollut.*, 218, pp.102-110,
491 <https://doi.org/10.1016/j.envpol.2016.08.036>, 2016.

492

493 Cheng J, Schloerke B, Karambelkar B, Xie Y, Aden-Buie G. *leaflet: Create Interactive Web Maps with the JavaScript*
494 *'Leaflet' Library*. R package version 2.2.3.9000, <https://rstudio.github.io/leaflet/>, 2025

495

496 Cliff, S.J., Drysdale, W., Lewis, A.C., Møller, S.J., Helfter, C., Metzger, S., Liddard, R., Nemitz, E., Barlow, J.F. and Lee, J.
497 D., Evidence of Heating-Dominated Urban NO_x Emissions. *Environ. Sci. Technol.* 59(9), pp.4399-4408.
498 <https://doi.org/10.1021/acs.est.4c13276>, 2025

499

500 Defratyka, S.M., Paris, J.D., Yver-Kwok, C., Fernandez, J.M., Korben, P. and Bousquet, P., Mapping urban methane sources
501 in Paris, France. *Environ. Sci. Technol.*, 55(13), pp.8583-8591. <https://doi.org/10.1021/acs.est.1c00859>, 2021

502

503 Department for Energy Security and Net Zero (DESNZ), Energy Trends: Natural Gas, Energy Trends September 2024,
504 https://assets.publishing.service.gov.uk/media/66f423473b919067bb48270e/Energy_Trends_September_2024.pdf (accessed
505 December 2024), 2024

506

507 Department for Transport: Road Length Statistics, RDL0102: Road length (miles) by road type and local authority in Great
508 Britain, <https://www.gov.uk/government/statistical-data-sets/road-length-statistics-rdl> (accessed April 2025), 2025

509

510 Dowd, E., Manning, A.J., Orth-Lashley, B., Girard, M., France, J., Fisher, R.E., Lowry, D., Lanoisellé, M., Pitt, J.R.,
511 Stanley, K.M., O'Doherty, S., Young, D., Thistlethwaite, G., Chipperfield, M.P., Gloor, E. and Wilson, C., First validation
512 of high-resolution satellite-derived methane emissions from an active gas leak in the UK. *Atmos. Meas. Tech.*, 17(5),
513 pp.1599–1615. <https://doi.org/10.5194/amt-17-1599-2024>, 2024.

514

515 Energy Institute, Statistical Review of World Energy, Natural gas consumption in the United Kingdom (UK) from 2003 to
516 2023 (in billion cubic meters),
517 https://www.energyinst.org/_data/assets/pdf_file/0004/1055542/EI_Stat_Review_PDF_single_3.pdf (accessed December
518 2024), 2023.

519

520 Essex Planning Officers Association, The Essex Design Guide, Design Details, 2018 Edition, V3,
521 <https://www.essexdesignguide.co.uk/media/2402/design-details-v3.pdf> (Accessed December 2024), 2018.
522

523 European Commission, United States of America, Global methane pledge,
524 <https://www.ccacoalition.org/sites/default/files/resources//Global%20Methane%20Pledge.pdf> (accessed July 2025), 2021
525

526 Fernandez, J.M., Maazallahi, H., France, J.L., Menoud, M., Corbu, M., Ardelean, M., Calcan, A., Townsend-Small, A., van
527 der Veen, C., Fisher, R.E. and Lowry, D., Street-level methane emissions of Bucharest, Romania and the dominance of
528 urban wastewater. *Atmos. Environ-X*, 13, p.100153. <https://doi.org/10.1016/j.aeaoa.2022.100153>, 2022.
529

530 Hopkins, F. M.; Kort, E. A.; Bush, S. E.; Ehleringer, J. R.; Lai, C. T.; Blake, D. R.; Randerson, J. T. Spatial patterns and
531 source attribution of urban methane in the Los Angeles Basin. *J. Geophys. Res.: Atmos.* 121 (5), 2490– 2507,
532 <https://doi.org/10.1002/2015JD024429>, 2016.
533

534 IPCC, 2021: Climate Change 2021: The Physical Science Basis. Contribution of Working Group I to the Sixth Assessment
535 Report of the Intergovernmental Panel on Climate Change [Masson-Delmotte, V., P. Zhai, A. Pirani, S.L. Connors, C. Péan,
536 S. Berger, N. Caud, Y. Chen, L. Goldfarb, M.I. Gomis, M. Huang, K. Leitzell, E. Lonnoy, J.B.R. Matthews, T.K. Maycock,
537 T. Waterfield, O. Yelekçi, R. Yu, and B. Zhou (eds.)]. Cambridge University Press, Cambridge, United Kingdom and New
538 York, NY, USA, In press, <https://doi.org/10.1017/9781009157896>, 2021.
539

540 Joo, J., Jeong, S., Shin, J. and Chang, D.Y., Missing methane emissions from urban sewer networks. *Environ. Pollut.*, 342,
541 p.123101. <https://doi.org/10.1016/j.envpol.2023.123101>, 2024.
542

543 Keyes, T., Ridge, G., Klein, M., Phillips, N., Ackley, R. and Yang, Y., An enhanced procedure for urban mobile methane
544 leak detection. *Heliyon*, 6(10). <https://doi.org/10.1016/j.heliyon.2020.e04876>, 2020.
545

546 Lowry, D., Fisher, R. E., France, J. L., Coleman, M., Lanoisellé, M., Zazzeri, G., Nisbet, E. G., Shaw, J. T., Allen, G., Pitt,
547 J., and Ward, R. S.: Environmental baseline monitoring for shale gas development in the UK: Identification and geochemical
548 characterisation of local source emissions of methane to atmosphere, *Sci. Total Environ.*, 708, 134600,
549 <https://doi.org/10.1016/j.scitotenv.2019.134600>, 2020
550

551 Luetschwager, E., von Fischer, J.C. and Weller, Z.D., Characterizing detection probabilities of advanced mobile leak
552 surveys: Implications for sampling effort and leak size estimation in natural gas distribution systems. *Elem. Sci. Anth.*, 9(1),
553 p.00143. <https://doi.org/10.1525/elementa.2020.00143>, 2021.

554

555 Maazallahi, H., Fernandez, J.M., Menoud, M., Zavala-Araiza, D., Weller, Z.D., Schwietzke, S., Von Fischer, J.C., Denier
556 Van Der Gon, H. and Röckmann, T., Methane mapping, emission quantification, and attribution in two European cities:
557 Utrecht (NL) and Hamburg (DE). *Atmos. Chem. Phys.*, 20(23), pp.14717-14740. [https://doi.org/10.5194/acp-20-14717-](https://doi.org/10.5194/acp-20-14717-2020)
558 [2020](https://doi.org/10.5194/acp-20-14717-2020), 2020.

559

560 National Atmospheric Emissions Inventory (NAEI), UK Emissions Data Selector,
561 <https://naei.energysecurity.gov.uk/data/data-selector> . Selected emissions data for the year 2022, methane emissions related
562 to gas leakage from gas distribution 1B2b5. (accessed June 2025)

563

564 Nisbet, E.G., Manning, M.R., Lowry, D., Fisher R.E., Lan, X., Michel, S.E., France, J.L., Nisbet, R.E.R, Bakkaloglu, S.,
565 Leitner, S.M., Brooke, C., Röckmann, T., Allen, G., Denier van der Gon, H.A.C, Merbold, L., Scheutz, C., Woolley Maisch,
566 C., Nisbet-Jones, P.B.R., Alshalan, A., Fernandez, J.M. and Dlugokencky, E.J., Practical paths towards quantifying and
567 mitigating agricultural methane emissions, *Proceedings of the Royal Society A: Mathematical, Physical and Engineering*
568 *Sciences*, 481, 20240390, <https://doi.org/10.1098/rspa.2024.0390>, 2025

569

570 Phillips, N.G., Ackley, R., Crosson, E.R., Down, A., Hutyra, L.R., Brondfield, M., Karr, J.D., Zhao, K. and Jackson, R.B.,
571 Mapping urban pipeline leaks: Methane leaks across Boston. *Environ. Pollut.*, 173, pp.1-4.
572 <https://doi.org/10.1016/j.envpol.2012.11.003>, 2013.

573

574 Saunio, M., Martinez, A., Poulter, B., Zhang, Z., Raymond, P. A., Regnier, P., Canadell, J. G., Jackson, R. B., Patra, P. K.,
575 Bousquet, P., Ciais, P., Dlugokencky, E. J., Lan, X., Allen, G. H., Bastviken, D., Beerling, D. J., Belikov, D. A., Blake, D.
576 R., Castaldi, S., Crippa, M., Deemer, B. R., Dennison, F., Etiope, G., Gedney, N., Höglund-Isaksson, L., Holgerson, M. A.,
577 Hopcroft, P. O., Hugelius, G., Ito, A., Jain, A. K., Janardanan, R., Johnson, M. S., Kleinen, T., Krummel, P. B., Lauerwald,
578 R., Li, T., Liu, X., McDonald, K. C., Melton, J. R., Mühle, J., Müller, J., Murguia-Flores, F., Niwa, Y., Noce, S., Pan, S.,
579 Parker, R. J., Peng, C., Ramonet, M., Riley, W. J., Rocher-Ros, G., Rosentreter, J. A., Sasakawa, M., Segers, A., Smith, S. J.,
580 Stanley, E. H., Thanwerdas, J., Tian, H., Tsuruta, A., Tubiello, F. N., Weber, T. S., van der Werf, G. R., Worthy, D. E. J., Xi,
581 Y., Yoshida, Y., Zhang, W., Zheng, B., Zhu, Q. and Zhuang, Q., Global Methane Budget 2000 - 2020, *Earth Syst. Sci. Data*,
582 17, 1873-1958, <https://doi.org/10.5194/essd-17-1873-2025>, 2025.

583

584 Scarpelli, T.R., Jacob, D.J., Grossman, S., Lu, X., Qu, Z., Sulprizio, M.P., Zhang, Y., Reuland, F., Gordon, D. and Worden,
585 J.R., Updated Global Fuel Exploitation Inventory (GFEI) for methane emissions from the oil, gas, and coal sectors:
586 evaluation with inversions of atmospheric methane observations. *Atmos. Chem. Phys.*, 22(5), pp.3235-3249.
587 <https://doi.org/10.5194/acp-22-3235-2022>, 2022.

588

589 Sotoodeh, K., Why packing adjustment cannot stop leakage: Case study of a ball valve failing to seal after packing
590 adjustment during fugitive emission as per ISO 15848–1. *Eng. Fail. Anal.*, 130, p.105751.
591 <https://doi.org/10.1016/j.engfailanal.2021.105751>, 2021.
592
593 Stewart I., Bolton P.; Households off the gas-grid and prices for alternative fuels; House of Commons Library,
594 <https://researchbriefings.files.parliament.uk/documents/CBP-9838/CBP-9838.pdf> (accessed December 2024), 2024.
595
596 Symonds, J, August 15 2017, On Instrument Time Response: What it means, what it isn't, and why it matters, [Article],
597 LinkedIn. <https://www.linkedin.com/pulse/instrument-time-response-what-means-why-matters-jonathan-symonds/>
598 (Accessed November 2024)
599
600 Tettenborn J., Zavala-Araiza D., Stroeken, D., Maazallahi, H., van der Veen, C., Hensen, A., Velzeboer, I., van den Bulk, P.,
601 Gillespie, L., Ars, S., France, J., Lowry, D., Fisher, R. and Röckmann, T., Improving consistency in methane emission
602 quantification from the natural gas distribution systems across measurement devices. *Atmos. Meas. Tech.*, 18, 3569–3584,
603 <https://doi.org/10.5194/amt-18-3569-2025>, 2025
604 Ueyama, M., Umezawa, T., Terao, Y., Lunt, M. and France, J.L., Evaluating urban methane emissions and their attributes in
605 a megacity, Osaka, Japan, via mobile and eddy covariance measurements. *Atmos. Chem. Phys.*, 25(19), pp.12513–12534.
606 <https://doi.org/10.5194/acp-25-12513-2025>, 2025.
607 Umezawa, T., Terao, Y., Ueyama, M., Kameyama, S., Lunt, M. and France, J.L., Measurement report: Mobile measurements
608 to estimate urban methane emissions in Tokyo. *Atmos. Chem. Phys.*, 25(23), pp.18015–18029. [https://doi.org/10.5194/acp-](https://doi.org/10.5194/acp-25-18015-2025)
609 [25-18015-2025](https://doi.org/10.5194/acp-25-18015-2025), 2025.
610 Vogel, F., Ars, S., Wunch, D., Lavoie, J., Gillespie, L., Maazallahi, H., Röckmann, T., Neçki, J., Bartyzel, J., Jagoda, P. and
611 Lowry, D., Ground-Based Mobile Measurements to Track Urban Methane Emissions from Natural Gas in 12 Cities across
612 Eight Countries. *Environ. Sci. Technol.*, 58(5), pp.2271-2281. <https://doi.org/10.1021/acs.est.3c03160>, 2024.
613
614 von Fischer, J.C., Cooley, D., Chamberlain, S., Gaylord, A., Griebenow, C.J., Hamburg, S.P., Salo, J., Schumacher, R.,
615 Theobald, D. and Ham, J., Rapid, vehicle-based identification of location and magnitude of urban natural gas pipeline
616 leaks. *Environ. Sci. Technol.*, 51(7), pp.4091-4099. <https://doi.org/10.1021/acs.est.6b06095>, 2017.
617
618 Wagner, R. L., Farren, N. J., Davison, J., Young, S., Hopkins, J. R., Lewis, A. C., Carslaw, D. C., and Shaw, M. D.:
619 Application of a mobile laboratory using a selected-ion flow-tube mass spectrometer (SIFT-MS) for characterisation of

620 volatile organic compounds and atmospheric trace gases, *Atmos. Meas. Tech.*, 14, 6083–6100, [https://doi.org/10.5194/amt-](https://doi.org/10.5194/amt-14-6083-2021)
621 [14-6083-2021](https://doi.org/10.5194/amt-14-6083-2021), <https://doi.org/10.5194/amt-14-6083-2021>, 2021.

622

623 Weller, Z.D., Yang, D.K. and von Fischer, J.C., An open source algorithm to detect natural gas leaks from mobile methane
624 survey data. *PLoS One*, 14(2), p.e0212287. <https://doi.org/10.1371/journal.pone.0212287>, 2019.

625

626 Weller, Z.D., Im, S., Palacios, V., Stuchiner, E. and von Fischer, J.C., Environmental injustices of leaks from urban natural
627 gas distribution systems: patterns among and within 13 US metro areas *Environ. Sci. Technol.*, 56(12), pp.8599-8609.
628 <https://doi.org/10.1021/acs.est.2c00097>, 2022.

629

630 Wietzel, J.B. and Schmidt, M., Methane emission mapping and quantification in two medium-sized cities in Germany:
631 Heidelberg and Schwetzingen. *Atmos. Environ.-X*, 20, p.100228. <https://doi.org/10.1016/j.aecaoa.2023.100228>, 2023.

632

633 Yacovitch, T.I., Herndon, S.C., Roscioli, J.R., Floerchinger, C., McGovern, R.M., Agnese, M., Pétron, G., Kofler, J.,
634 Sweeney, C., Karion, A. and Conley, S.A., Demonstration of an ethane spectrometer for methane source
635 identification. *Environ. Sci. Technol.*, 48(14), pp.8028-8034. <https://doi.org/10.1021/es501475q>, 2014.